ADVANCED MATERIALS
www.advmat.de

Insulator Polymer Matrix Construction on All-Small-Molecule Photoactive Blend Towards Extrapolated 15000 Hour T_{80} Stable Devices

Ruijie Ma, Xinyu Jiang, Top Archie Dela Peña, Wei Gao, Jiaying Wu, Mingjie Li, Stephan V. Roth, Peter Müller-Buschbaum, and Gang Li**

To boost the stability of all-small-molecule (ASM) organic photovoltaic (OPV) blends, an insulator polymer called styrene-ethylene-butylene-styrene (SEBS) as morphology stabilizer is applied into the host system of small molecules BM-ClEH:BO-4Cl. Minor addition of SEBS (1 mg/ml in host solution) provides a significantly enhanced T_{80} value of 15000 hours (extrapolated), surpassing doping-free (0 mg/ml) and heavy doping (10 mg/ml) counterparts (900 hours, 30 hours). The material reproducibility and cost-effectiveness of the active layer will not be affected by this industrially available polymer, where the power conversion efficiency (PCE) can be well maintained at 15.02%, which is still a decent value for non-halogen solvent-treated ASM OPV. Morphological and photophysical characterizations clearly demonstrate SEBS's pivotal effect on suppressing the degradation of donor molecules and blend film's crystallization/aggregation reorganization, which protects the exciton dynamics effectively. This work pays meaningful attention to the ASM system stability, performs a smart strategy to suppress the film morphology degradation, and releases a comprehensive understanding of the mechanism of device performance reduction.

1. Introduction

Developing new energy generation technologies is of fundamental importance to have carbon neutrality realized. Organic photovoltaic (OPV) devices are among the most promising candidates, due to their unreplaceable advantages of lightweight and semi-transparent.[1–15] OPVs based on polymers as photoactive materials constantly suffer from batch-to-batch differences of the conjugated polymers, which seriously decrease the reproducibility and increases the fabrication costs.[16–20] Hence, developing solar cells based on all-small-molecule (ASM) active layers is a rational way to realize both, efficient and cost-effective OPVs.[21–30] However, ASM systems generally demonstrate poorer operational stability than their polymer-counterparts, because of a more fragile molecular packing and aggregation.[31] Hence,

R. Ma, G. Li
Department of Electrical and Electronic Engineering
Research Institute for Smart Energy (RISE)
Photonic Research Institute (PRI)
The Hong Kong Polytechnic University
Hong Kong China
E-mail: ruijie.ma@polyu.edu.hk; gang.w.li@polyu.edu.hk

X. Jiang, S. V. Roth
Deutsches Elektronen-Synchrotron (DESY)
Notkestraße 85, 22607 Hamburg, Germany

T. A. Dela Peña, J. Wu
Advanced Materials Thrust
Function Hub
The Hong Kong University of Science and Technology
Nansha, Guangzhou China

T. A. Dela Peña, M. Li
Department of Applied Physics
The Hong Kong Polytechnic University
Hong Kong China

W. Gao
Xiamen Key Laboratory of Optoelectronic Materials and Advanced Manufacturing
Institute of Luminescent Materials and Information Displays
College of Materials Science and Engineering
Huaqiao University
Xiamen 361021, China

S. V. Roth
Fibre and Polymer Technology
KTH Royal Institute of Technology
Stockholm 10044, Sweden

P. Müller-Buschbaum
TUM School of Natural Sciences
Department of Physics
Chair for Functional Materials
Technical University of Munich
James-Franck-Str. 1, 85748 Garching, Germany

The ORCID identification number(s) for the author(s) of this article can be found under https://doi.org/10.1002/adma.202405005

DOI: 10.1002/adma.202405005

promoting the ASM blend stability is of great significance to the field development.

As a direct comparison, polymer donors and acceptors (PD and PA) with higher glass transition temperatures (Tg) and interconnected networks in films demonstrate superior morphology stability compared to those of small molecule donors and acceptors (SMD and SMA).[32–36] Thereby, endowing ASM active layer polymer-like morphological features is a practical way to realize an improved device stability. For instance, Wei and coworkers realized applying PA into the ASM system to boost the efficiency and stability.[37,38] The disadvantage of this strategy is incorporating PA or PD with synthetic difficulties and batch-to-batch performance variations would undermine the significance of developing ASM systems. On the other hand, industrially produced insulator polymers like polystyrene (PS) and styrene-ethylene-butylene-styrene (SEBS), were noticed by researchers. They were applied to PD:SMA systems to promote their mechanical stability, thickness tolerance, as well as power conversion efficiency (PCE).[39–45] Notably, insulating polymers such as SEBS are widely available through commercial products with cheap prices, and high production reproducibility. Thereby, exploiting the potential morphology stabilizing effect of these insulators in ASM based active layers will be an ideal way to address the stability enhancement and reproducibility protection.

In the present study, SEBS is chosen to be incorporated into a green solvent processable ASM system called BM-ClEH:BO-4Cl.[46] The addition of SEBS generally reduces the PCE from 15.72% to 15.01% (1 mg/ml), 14.84% (2 mg/ml), 13.51% (5 mg/ml), and 5.62% (10 mg/ml). The initial efficiency drop is due to the loss from short-circuit current density (J_{SC}) and fill factor (*FF*), which is consistent with former research on insulator doping topics.[40,47] For low-concentration SEBS doping (1 mg/ml and 2 mg/ml), the efficiency reduction is marginal, where J_{SC} loss is significant, but *FF* varies little, and open-circuit voltage (V_{OC}) becomes even higher due to a blue-shifted photon response of the devices. For higher SEBS content, the loss of *FF* and J_{SC} are highly recognizable, which is suggested to be the results of pure SEBS agglomerates showing up. Subsequently, the device stabilities of doping-free (0 mg/ml), minor doping (1 mg/ml), and strong doping (10 mg/ml) under maximal power point (MPP) tracking mode are investigated. The simple ASM device and 10 mg/ml SEBS doped one display continuous PCE losses in the whole MPP tracking, while minor SEBS (1 mg/ml) treated ASM OPV demonstrates a stabilized energy output after the burn-in loss. The calculated estimation of the optimal device lifetime T_{80} (the time at which the PCE of the solar cell has reached 80% of its original value) value is 15000 hours. This is a decent performance progress for ASM systems, which is comparable to those realized by PD:PA/giant molecule acceptor (GMA) combinations.[35,48–53] The morphological analyses reveal that 1 mg/ml SEBS doping in solution leads to stabilized π-π stacking and phase separation states, so better-kept charge generation and transport tunnels. Moreover, photophysical testing suggest that SEBS containing active layers demonstrate a more stable singleton decay and polaron generation/extinction kinetics. The poor stability in the control system is driven by BM-ClEH's (SMD) crystallization evolution and aggregation relaxation. For 10 mg/ml SEBS doped blend films, large insulating agglomerates, poor dielectric coefficient, and destroyed contact between active layer and charge transport layer are taken as rational explanations on the poorest efficiency and stability. Our study reports an effective way to improve the stability of ASM systems without sacrificing its material reproducibility or cost effectiveness, and presents in-depth morphological and photophysical understandings for active layer's photoinduced degradation.

Table 1. Photovoltaic performance of BM-ClEH:BO-4Cl blend based ASM devices.

SEBS content	V_{OC} [V]	J_{SC} [mA cm^{-2}]	*FF* [%]	PCE [%]
0 mg/ml	0.856	24.75/24.12	74.2	15.72
1 mg/ml	0.859	23.55/22.93	74.2	15.01
2 mg/ml	0.865	23.67/23.27	72.5	14.84
5 mg/ml	0.861	22.57/22.11	69.5	13.51
10 mg/ml	0.858	13.81/13.68	47.4	5.62

2. Results and Discussion

Here, the ASM system chosen as a reported green solvent processable SMD:SMA pair is BM-ClEH:BO-4Cl, which chemical structures are shown in **Figure 1**a, together with that of SEBS. While BM-ClEH was synthesized in former work, and BO-4Cl is bought from a supplier, the source of SEBS is demonstrated by Figure S1: A large-scale produced by a company. The proposed morphology changes introduced by SEBS incorporation are sketched in Figure 1b. The SMD:SMA molecular packing and phase distribution was revealed before.[46] It was concluded to be a strongly crystalline and aggregated donor-acceptor interpenetrating network. The role of SEBS in the treated films can be divided into two aspects: (i) The chain relaxation leads to a fibrillar polymeric structure located at an amorphous region, which is beneficial to suppressing undesired molecule diffusion, thus stabilizing the morphology; (ii) self-entangled polymer formed agglomerates that may on the one hand be resistive to external stress led morphology degradation, and on the other hand negatively affect original charge generation and transport between donor and acceptor phases.

Subsequently, the devices based on the BM-ClEH:BO-4Cl (ASM) system processed with different concentrations of SEBS are fabricated to evaluate the performance variation with a conventional device structure of ITO/PEDOT:PSS/active layer/PFN-Br/Ag.[54] Figure 1c shows the current density versus voltage (*J-V*) characteristics. Related parameters are extracted and summarized in **Table 1**. It is recognizable that SEBS incorporation at a low concentration does not destroy the PV performance, although it is a high molecular weight insulator polymer. The efficiency drop is driven by a reduced J_{SC} and *FF*, while the V_{OC} values of SEBS treated devices are all higher than the control. Accordingly, the 1 mg/ml SEBS doped system exhibits a 15.01% PCE, slightly lower than the reference binary solar cells (15.72%), which stands for a state-of-the-art level of green solvent processed ASM OPV still. When the concentration of SEBS comes to 10 mg/ml in THF solution, PCE suffers a great loss due to drastically reduced J_{SC} and *FF* values. Hence, there are three kinds

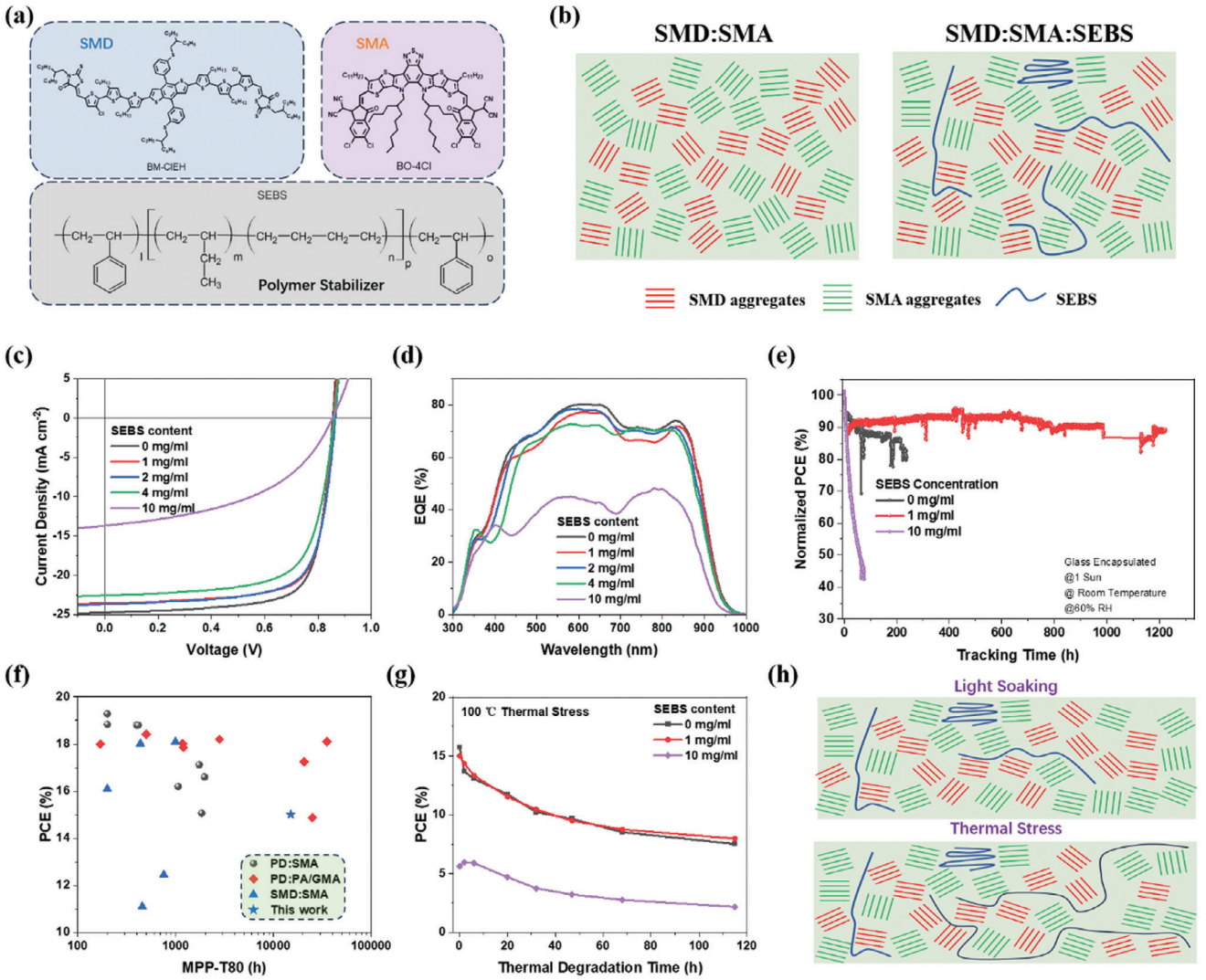

Figure 1. a) Chemical structure of BM-ClEH, BO-4Cl, and SEBS. b) Schematic diagrams of the morphology upon adding SEBS. c) *J-V* characteristics of BM-ClEH:BO-4Cl based solar cells with different SEBS concentrations. d) EQE spectra of related devices. e) MPP tracking curves of studied devices. f) Summary of recent progress on OSC device efficiencies and stabilities for PD:SMA, PD:PA/GMA, and SMD:SMA types of systems. g) Thermal stability of BM-ClEH:BO-4Cl:SEBS photovoltaic blends. h) Schematic diagram of morphology evolution under light and thermal treatments.

of active layers in this work: doping-free, low-degree doping, and high-degree doping. The external quantum efficiency (EQE) measurements are simultaneously carried out to assure the efficiency accuracy. The acquired spectra and integrated current density values are displayed in Figure 1d and Table 1, respectively. The results suggest that measurement errors of this study are controlled within 3%.

Next, the device stability of doping-free, low-degree doping, and high-degree doping systems (0 mg/ml SEBS, 1 mg/ml SEBS, 10 mg/ml SEBS) is investigated by maximal power point (MPP) tracking upon corresponding glass encapsulated devices, under one sun (simulated), room temperature (~25 °C), and 60% relative humidity conditions.[55] The recorded PCE versus time curves are plotted in Figure 1e. Both control and low-degree doping cells demonstrate acceptable operational devices. However, the T_{80} value of 1 mg/ml SEBS treated devices is much larger than that of the control. On the other hand, devices made from the 10 mg/ml SEBS doped system display poor stability, due to a nearly linear performance drop. These results indicate that low-degree doping can significantly prolong the device lifetime without sacrificing too much initial PCE, while high-degree doping only leads to poor efficiency and low stability. Moreover, during the MPP tracking period, the optimal device efficiency has not degraded to the level of less than 80% of initial value. Thus, an extrapolated T_{80} value of 15000 hours is calculated, which is a decent lifetime in OPVs, especially for those based on ASM systems. To better show the significance and compare with other OPV works, an efficiency-stability summary graph is comprised as Figure 1f, generated by the data source given in Table S1. As shown here, the comprehensive performance of 1 mg/ml SEBS doped BM-ClEH:BO-4Cl system is comparable to what was achieved by PD:PA and PD:GMA blends. Considering the

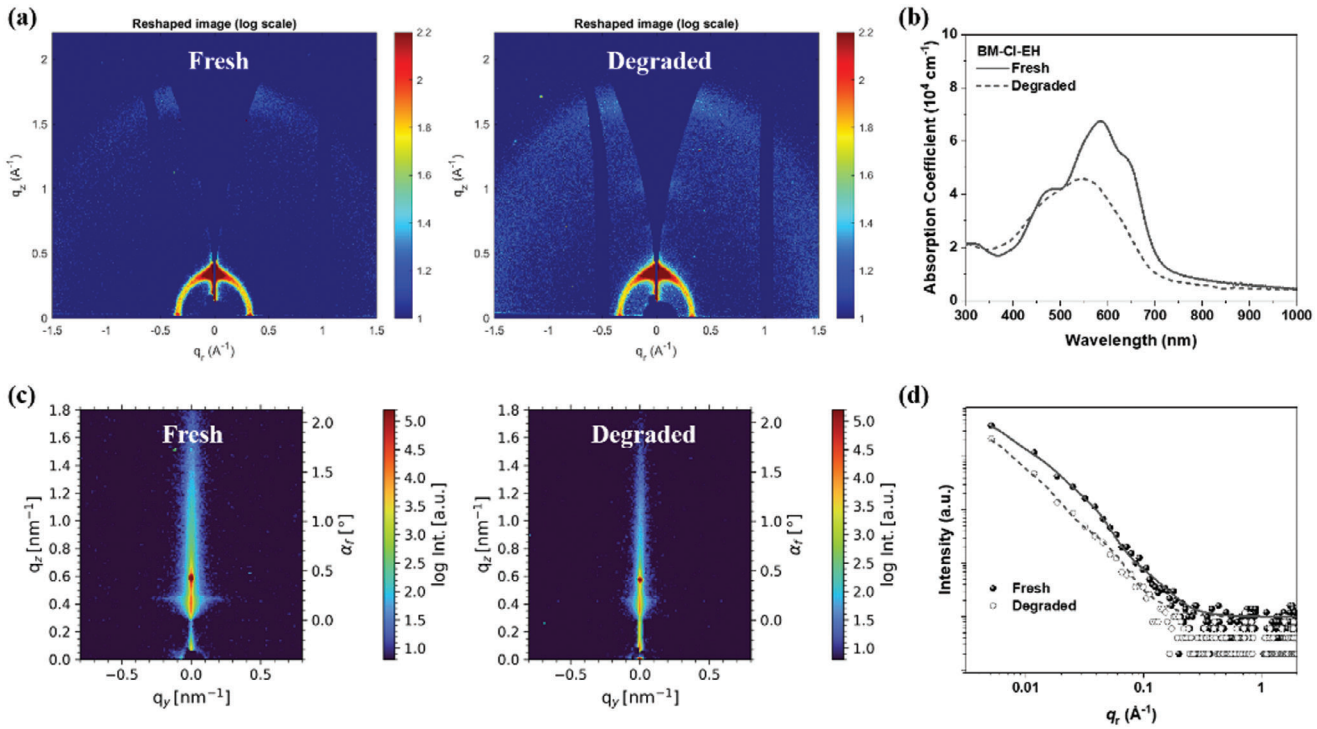

Figure 2. a) 2D GIWAXS data, b) UV-vis absorption spectra, c) 2D GISAXS data, and d) IP intensity line-cuts & fits of fresh and degraded BM-ClEH neat films.

synthetic reproducibility, our solar cell would be even more competitive. Meanwhile, the scalability of SEBS production up to kilogram or ton's scale guarantee the system won't suffer polymer's batch to batch performance variation.

In addition, the thermal stability of the devices is also evaluated by placing them on a 100 °C hotplate in a nitrogen atmosphere. The results summarized by Figure 1g imply that SEBS incorporation brings no significant stability enhancement or reduction for the control ASM system. This finding might be due to several factors: (i) the p-i-n device architecture with PEDOT:PSS and PFN-Br cannot produce thermally tolerant charge transport layers; (ii) ASM systems without nanofibrillar network and of low Tg value cannot endure serious thermal stress; (iii) the morphology evolution of donor-acceptor phases, as well as the aggregation behavior of SEBS in film driven by sunlight illumination and annealing is supposed to be different, as indicated by Figure 1h, where SEBS's chain relaxation or induced agglomeration may not be helpful to maintaining the device efficiency under thermal stress compared to light soaking condition. Thereby, the following morphology and device physics investigations focus on ASM active layer's photodegradation.

To comprehensively evaluate the morphology changes caused by illumination, fresh and photo-degraded (for 200 hours) samples of neat and blend films are all screened by different characterization techniques, including grazing incidence wide-angle X-ray scattering (GIWAXS), grazing incidence small-angle X-ray scattering (GISAXS), and ultraviolet-visible (UV-vis) absorption spectroscopy. These investigations provide a complete illustration of the active layer crystallization behavior and aggregation state evolution.[56–62] As demonstrated by **Figure 2**a, the 2D GIWAXS data of neat SMD films in fresh and degraded states, directly indicate that light soaking leads to enhanced in-plane (IP) lamellar and out-of-plane (OOP) π–π stacking signals, according to Figure S2 and extracted parameters in Tables S2 and S3. It can be then inferred that BM-ClEH neat film crystallinity is enhanced after light degradation, whereas its π–π stacking is loosened. Next, the light absorbing ability (characteristic) is investigated through UV-vis spectra of fresh and degraded samples. Figure 2b obviously shows that degraded SMD has no significant H-aggregation correlated absorption peaks.[46] This optical degradation is empirically negative to keep the initial device performance. On the other hand, increased crystallinity and reduced light harvesting ability imply that in the aged film, aggregation mode and phase length scale shall be altered significantly. Hence, further analysis based on GISAXS is carried out, as presented in Figure 2c,d, that includes 2D patterns and IP directional intensity line-cuts, as well as fits to the data. Corresponding calculated phase separation parameters are summarized in Table S4. Accordingly, light soaking induces a significant increase in small-scale domains compared with the fresh film. This large amount of small crystalline phases disconnect from each other, thus destroying the initial aggregation motif and fibrillar network.

In addition, the same investigations are applied to BO-4Cl fresh and degraded neat films. Obtained results are displayed in Figures S3 and S4, and Tables S2–S4. These results indicate that the SMA used here has a significantly better photo-stability: The molecular packing distance (d-spacing), orientation, crystalline coherence length (CL), absorption profile, and phase separation scale values are rarely changed after degradation. Thereby, it can be further concluded that the ASM photovoltaic blend

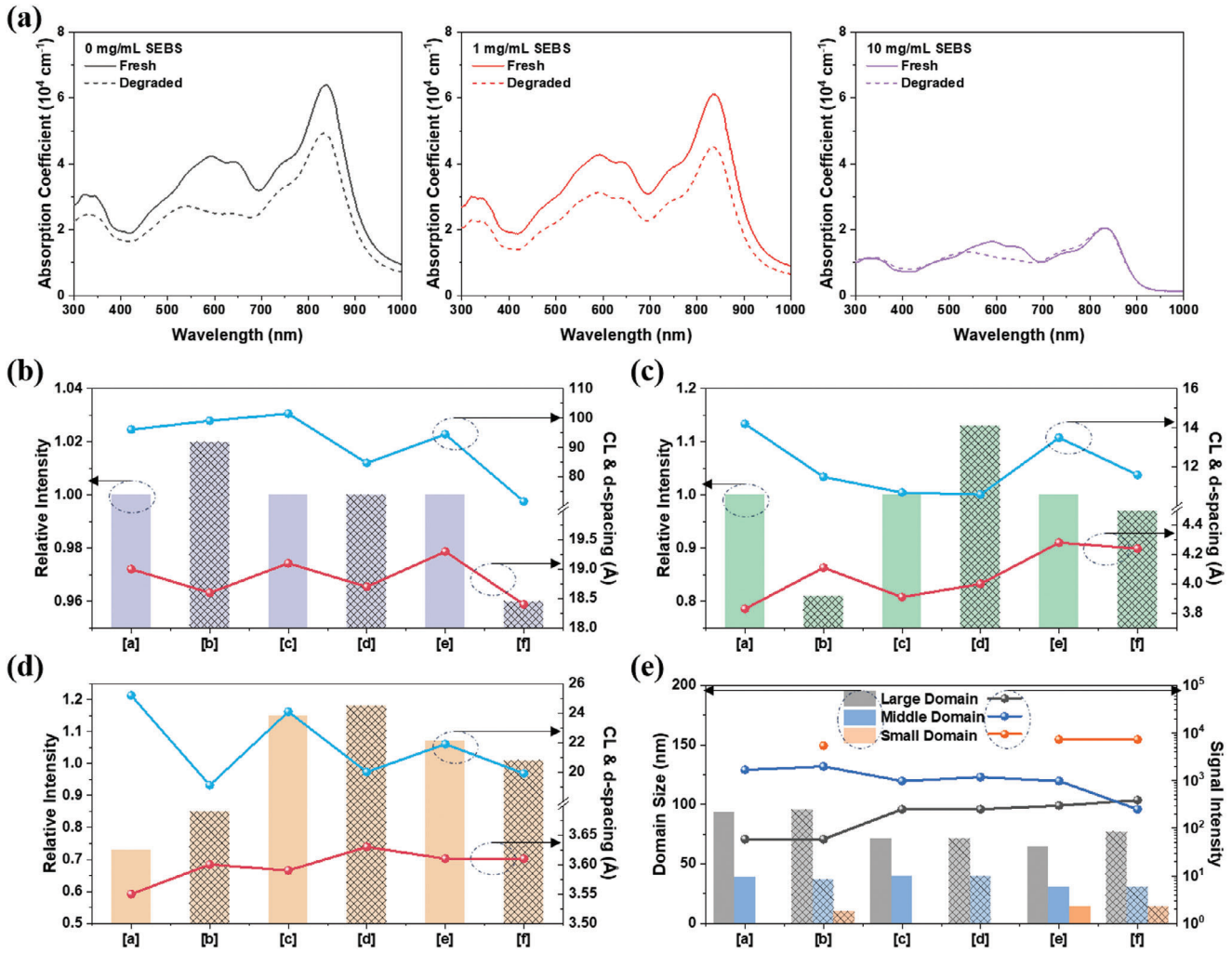

Figure 3. Blend film morphology investigations: a) UV-vis absorption spectra of fresh and degraded BM-ClEH:BO-4Cl systems with 0 mg/ml, 1 mg/ml, and 10 mg/ml SEBS concentration in blends. Calculated crystalline parameters for b) IP directional lamellar peaks, c) OOP directional π-π stacking vice peaks, and d) main peaks. e) Results from GISAXS data analysis, including domain sizes and related intensity values. Bottom axis labels [a] to [e] represent 0, 1 and 10 mg/ml SEBS fresh & degraded, respectively.

morphology degradation is mainly driven by SMDs changes. Besides, GIWAXS measurements are also applied to the neat films of SEBS, which reveals no crystalline structures solely contributed by it (Figure S5).

After figuring out the SMD-originated instability, the SEBS's incorporation in blend film-induced morphology change in fresh and degraded films is assessed by the same series of characterizations. The UV-vis spectra of blend films doped by 0 mg/ml, 1 mg/ml, and 10 mg/ml SEBS are presented in **Figure** 3a. Consistent with the neat film analyses, light-induced degradation mainly comes from the SMD, whose characteristic absorption peaks nearly vanish in binary control film after degradation, while the general profiles can be maintained in the 1 mg/ml SEBS treated BM-ClEH:BO-4Cl active layers. As for the 10 mg/ml SBES introduced system, the fresh film absorption ability is significantly reduced, which is supposed to be the result of too much insulating polymer agglomerates. Its aged film instead, demonstrates the most insignificant absorption reduction. Accordingly, the morphology stabilization effect of SEBS can be initially confirmed.

Subsequently, the crystalline features are one-by-one studied, as presented in Figure 3b–d, for IP's (100) peaks, IP (100) vice peaks, and OOP (010) main peaks, respectively. The original 2D GISAXS data and intensity line-cuts are given as Figures S6–S8. Beyond d-spacing and CL, the relative intensity is included as a parameter to assess the change of film crystallinity. From the data, one can easily realize that light soaking increases the IP directional lamellar packing's crystallinity and ordering, indicative of the formation of independent new crystalline phase with <10 nm size, which is consistent with analyzed results of the SMD neat film. With 1 mg/ml SEBS addition, the crystallinity change can be well suppressed, while an acceptable loss of CL is seen. As for the 10 mg/ml SEBS case, the active layer crystallinity demonstrates a recognizable reduction after illumination, implying that in this scenario, the crystallization of BM-ClEH molecules is suppressed by SEBS agglomeration.

The π–π stacking peaks of the blend films are all supposed to be mathematically treated as two merged peaks: vice and main that are due to the SMA's characteristics. Hence, the vice peak is also fitted as a supplementary description for the main peak results. Likewise, the crystallinity and crystalline ordering change of SEBS-treated films are suppressed. In addition, SEBS introduction makes the main peak higher than the vice peak, which could be the result of BO-4Cl's crystallization behavior alterations.

For further understanding of the inner film morphology, GISAXS measurements are conducted on blend films, as shown in Figure S9. Horizontal line cuts of the 2D GISAXS data at the Yoneda region and the corresponding fits performed based on a DWBA and EIA model (assuming three cylinder-type substructures: large, medium, and small domain sizes). The analyzed results are summarized in Figure 3e and Table S4. Similar to the BM-ClEH's neat films light-induced morphology changes, the degraded binary control system exhibits an intensity increase of the small domain signal, which implies a less continuous network characteristic. For 1 mg/ml SEBS-included systems, an insignificant phase separation behavior variation is found between the fresh and degraded films. In addition, the large amount of SBES (10 mg/ml) treated blend realizes a domain distribution with a clearer small-size signal. After the illumination, we can easily see the enlargement of the domain size and the intensity for the large-scale phases. Such experimental results suggest that a high concentration insulator polymer doping leads to a small molecule phase separation suppression. Moreover, light soaking further enhances the SEBS agglomeration. Overall, a stabilized morphology is realized for the ASM photoactive blend by adding 1 mg/ml SEBS.

We may notice that the 10 mg/ml SEBS treated active layer crystallization and phase separation behavior is also well maintained, however, the corresponding device has the poorest stability. This observation might be explained by a strongly reduced dielectric constant of the active layer at high-concentration SEBS addition. Alongside the MPP tracking, SEBS agglomerates could concentrate at the surface or bottom of the active layer. As a result, the conductivity of the device shall be much poorer than a normal photodiode requires.

Subsequently, the exciton splitting and charge recombination kinetics of fresh and aged films with or without SEBS treatment is explored by femto-second transient absorption spectroscopy (fs-TAS) experiments.[63–65] The SEBS doping effect on fresh device carrier kinetics is firstly evaluated by polaron generation and sub-ns recombination, as plotted in **Figure** 4a. The corresponding spectral line cuts and 2D pseudo contour maps are presented in Figure S10. The active layer of 1 mg/ml SEBS demonstrates almost identical recombination dynamics to the binary control, while the 10 mg/ml SEBS system exhibits significantly accelerated charge recombination, well consistent with the *FF* changing tendency. The addition of SEBS induces a faster polaron generation driven by a faster singlet exciton decay as shown by Figure 4b. In combination with the device parameter variation, the singlet exciton decay speeding up at higher SEBS concentration contributes to more severe geminate recombination losses, as most observable from the 10 mg/ml SEBS doped active layer. These characteristics are all supportive to the fresh device performance variations.[64,66]

Next, the comparison of fresh and degraded films on charge carrier dynamics is carried out, too. Based on raw data presented in Figure S11, Figure 4c again confirms that the degraded part of the ASM photoactive blend is mainly contributed by BM-ClEH (SMD): The ground state bleaching (GSB) peak of SMD is significantly blue-shifted after the light degradation, and its singlet exciton lifetime is decreased, which has just been confirmed detrimental by inducing more pronounced mono-molecular (geminate) recombination. On the contrary, BO-4Cl (SMA) based neat films before and after continuous illumination demonstrate no significant differences in the aspects of GSB peak position and singleton decay lifetime (Figure S11c). Moreover, the blend films after degradation are measured and analyzed in Figure S12, and Figure 4d–f. Herein, the blue-shift of the hole polarons photobleach (PB) peak is also observed in degraded films of 0 mg/ml and 10 mg/ml SEBS compared to their fresh samples, while only 1 mg/ml SEBS contained film has a stabilized PB peak characteristics after continuous illumination. Thereby, low content SEBS doping could enable either hole transfer from SMA to the stable SMD phase, or directly stabilized the SMD molecules. Furthermore, the exciton decay kinetics shown in Figure S12 support that 1 mg/ml SEBS contained system has the most insignificant change after degradation, which corresponds to the stabilized hole transfer process. As the hole transfer process requires suitable SMD morphology, this result also indicates 1 mg/ml SEBS in solution contributes to the film morphology's stabilization.

In addition, the general applicability of SEBS built insulator polymer matrix in active layers based on SMD:SMA material systems towards better stability is confirmed via other two systems, BTR-Cl:BO-4Cl and B1:BO-4Cl.[67,68] The conclusion that SMDs are the main degradation factor of active layer morphology and device performance is also proven here, as demonstrated by Figure S13: the normalized absorption profiles show the fast degradation of BTR-Cl and B1's characteristic aggregation induced peaks. Next, the photovoltaic performances including fresh device efficiencies and light soaking (1 sun) stability of control (binary) and 1 mg/ml SEBS included ASM OSCs based on these two active systems are demonstrated in Figure S14 and Table S5. The change tendency displayed hereby is similar to what has been found in BM-ClEH:BO-4Cl system in the main text.

3. Conclusion

In summary, to maintain the advantage of the ASM system, and to make up its stability performance, a cost-effective, highly reproducible, and ultra-stable insulator polymer, called SEBS is introduced into BM-ClEH:BO-4Cl's precursor based on THF as solvent. It results in an over 15% PCE for green solvent processed ASM OPV devices, and a decent MPP device T_{80} lifetime of ~15000 hours under 1 sun continuous illumination. Via a series of morphological and photophysical investigations on the fresh and degraded neat and blend films, the degradation motivation is revealed to be SMD material's unfavorable evolution of forming smaller scale crystalline domains, and destroying the D/A network. The incorporation of SEBS with a low content effectively suppresses this kind of undesirable morphology degradation and finally achieve satisfying device operational stability for ASM system, which contributes to the pursuit of carbon

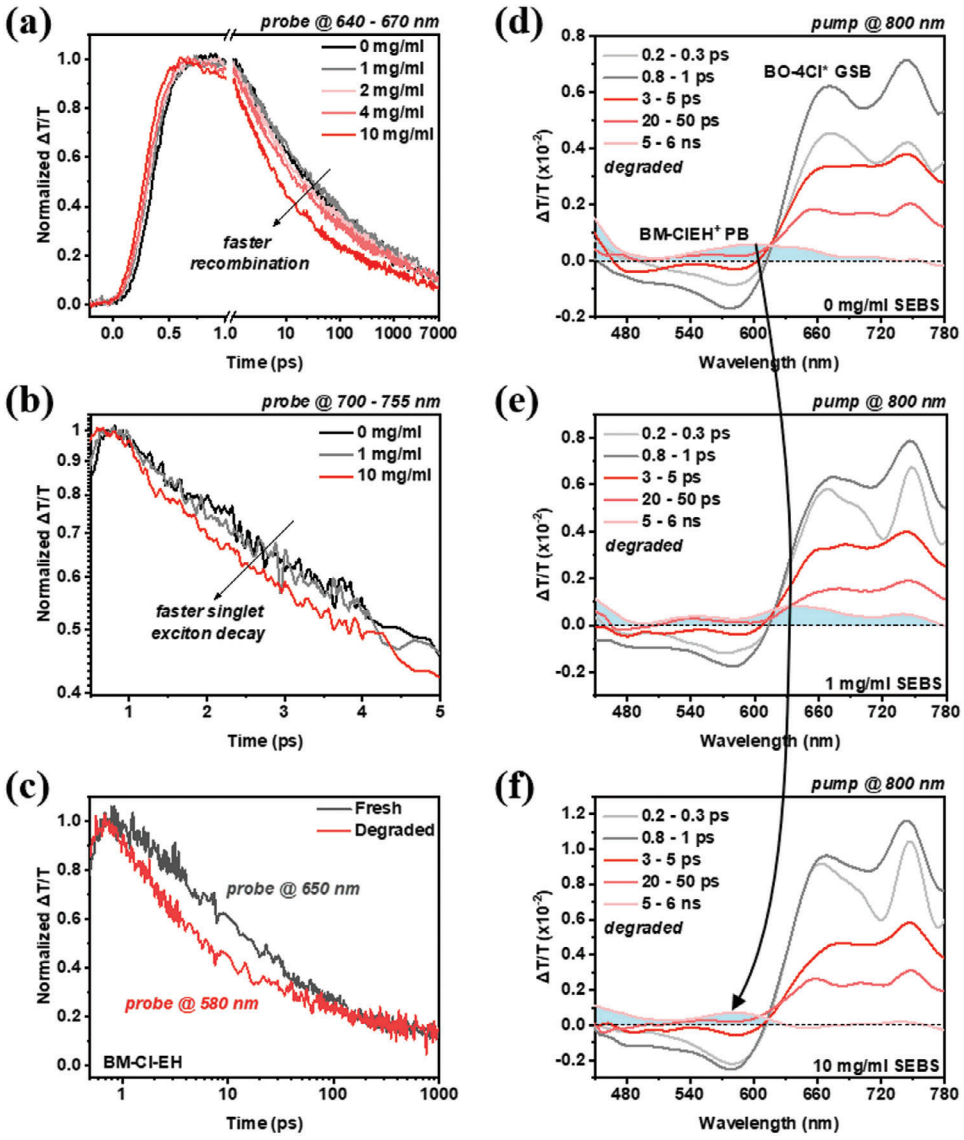

Figure 4. a) Polaron dynamics of fresh blend active layers with different SEBS concentration doping. b) Singlet exciton decay kinetics of blend fresh films with 0 mg/ml, 1 mg/ml, and 10 mg/ml SEBS. c) Comparison of fresh and degraded SMD film's singlet exciton decay kinetics. The selected probe wavelengths between fresh (650 nm) and degraded (580 nm) samples are different due to the absorption spectral peak changes upon degradation of BM-Cl-EH. TAS representative spectra of degraded ASM films with d) 0 mg/ml SEBS, e) 1 mg/ml SEBS, and f) 10 mg/ml SEBS. TAS measurements were performed using 800 nm pump wavelength at 5 μJ/cm^2 fluence. In the Tas spectral assignments, BO-4Cl* GSB corresponds to the ground state bleaching (GSB) of BO-4Cl singlet excitons, BO-4Cl* PIA corresponds to the photo-induced absorption (PIA) of BO-4Cl singlet excitons, and BM-C1EH$^+$ corresponds to the BM-C1EH hole polarons photobleach (PB).

neutrality.[69,70] Furthermore, in foreseeable future researches, some fluorine/chlorine functionalized insulating polymers can be utilized in similar scenarios, too, as their possibility on boosting device efficiency and stability simultaneously. This work not only presents an effective stability promotion strategy and a decent result but also demonstrates a systematic study and an in-depth understanding of active layer morphology change.

Supporting Information

Supporting Information is available from the Wiley Online Library or from the author.

Acknowledgements

R.M. thanks the support from PolyU Distinguished Postdoc Fellowship (1-YW4C). G.L. acknowledges the support from Research Grants Council of Hong Kong (Project Nos 15221320, 15307922, C7018-20G, C5037-18G, C4005-22Y), RGC Senior Research Fellowship Scheme (SRFS2223-5S01), Shenzhen Science and Technology Innovation Commission (JCYJ20200109105003940), the Hong Kong Polytechnic University: Sir Sze-yuen Chung Endowed Professorship Fund (8-8480), RISE (Q-CDBK), PRI (Q-CD7X), and Guangdong-Hong Kong-Macao Joint Laboratory for Photonic-Thermal-Electrical Energy Materials and Devices (GDSTC No. 2019B121205001). W.G. is grateful to the National Natural Science Foundation of China (U23A20371), the Scientific Research Funds of Huaqiao University (605-50Y23024). X.J. and S.V.R. acknowledge funding

by the Federal Institute for Research on Building, Urban Affairs and Spatial Development on behalf of the Federal Ministry of the Interior, Building and Community with funds from the Zukunft Bau research programme under grant "Nachhaltige Sonnenschutzsysteme aus hochfester Zellulose zur Umwandlung von Sonnenenergie" P.M.-B. acknowledges funding by Deutsche Forschungsgemeinschaft (DFG, German Research Foundation) under Germany´s Excellence Strategy – EXC 2089/1 – 390776260 (e-conversion) and via International Research Training Group 2022 Alberta/Technical University of Munich International Graduate School for Environmentally Responsible Functional Hybrid Materials (ATUMS)., as well as from TUM.solar in the context of the Bavarian Collaborative Research Project Solar Technologies Go Hybrid (SolTech).

Conflict of Interest

The authors declare no conflict of interest.

Author Contributions

R.M.: Conceptualization, Project Administration, Investigation, Formal Analysis, Methodology, Writing-Original Draft, X.J.: Investigation, Formal Analysis, Methodology, Writing-Review & Editing, T.A.D.P.: Investigation, Formal Analysis, Methodology, Writing-Review & Editing, W.G.: Investigation, Resources, Funding Acquisition, J.W.: Resources, M.L.: Resources, S.V.R.: Resources, Supervision, P.M.-B.: Resources, Funding Acquisition, Supervision, Writing—Review & Editing, G.L.: Supervision, Resources, Funding Acquisition

Data Availability Statement

The data that support the findings of this study are available from the corresponding author upon reasonable request.

Keywords

additive, all-small-molecule, morphology, organic photovoltaic, stability

Received: April 7, 2024
Revised: June 9, 2024
Published online: July 11, 2024

[1] Y. Liu, B. Liu, C.-Q. Ma, F. Huang, G. Feng, H. Chen, J. Hou, L. Yan, Q. Wei, Q. Luo, Q. Bao, W. Ma, W. Liu, W. Li, X. Wan, X. Hu, Y. Han, Y. Li, Y. Zhou, Y. Zou, Y. Chen, Y. Li, Y. Chen, Z. Tang, Z. Hu, Z.-G. Zhang, Z. Bo, *Sci China Chem* **2022**, *65*, 224.
[2] Y. Liu, B. Liu, C.-Q. Ma, F. Huang, G. Feng, H. Chen, J. Hou, L. Yan, Q. Wei, Q. Luo, Q. Bao, W. Ma, W. Liu, W. Li, X. Wan, X. Hu, Y. Han, Y. Li, Y. Zhou, Y. Zou, Y. Chen, Y. Liu, L. Meng, Y. Li, Y. Chen, Z. Tang, Z. Hu, Z.-G. Zhang, Z. Bo, *Sci China Chem* **2022**, *65*, 1457.
[3] H. Yu, J. Wang, Q. Zhou, J. Qin, Y. Wang, X. Lu, P. Cheng, *Chem. Soc. Rev.* **2023**, *52*, 4132.
[4] J. Wang, Q. Luan, P. Wang, C. Han, F. Bi, C. Yang, Y. Li, X. Bao, *Adv. Funct. Mater.* **2023**, *33*, 2301575.
[5] Z. Wang, X. Wang, L. Tu, H. Wang, M. Du, T. Dai, Q. Guo, Y. Shi, E. Zhou, *Angew. Chem., Int. Ed.* **2024**, *63*, 202319755.
[6] H. Zhu, Y. Li, *Green Carbon* **2023**, *1*, 14.
[7] R. Ma, X. Jiang, J. Fu, T. Zhu, C. Yan, K. Wu, P. Müller-Buschbaum, G. Li, *Energy Environ. Sci.* **2023**, *16*, 2316.
[8] T. Xu, B. Deng, Y. Zhao, Z. Wang, G. Lévêque, Y. Lambert, B. Grandidier, S. Wang, F. Zhu, *Adv. Energy Mater.* **2023**, *13*, 2301367.
[9] X. Dong, X. Zhou, Y. Liu, S. Xiong, J. Cheng, Y. Jiang, Y. Zhou, *Energy Environ. Sci.* **2023**, *16*, 1511.
[10] Y. Xin, H. Liu, X. Dong, Z. Xiao, R. Wang, Y. Gao, Y. Zou, B. Kan, X. Wan, Y. Liu, Y. Chen, *J. Am. Chem. Soc.* **2024**, *146*, 3363.
[11] W. Wei, C. e. Zhang, Z. Chen, W. Chen, G. Ran, G. Pan, W. Zhang, P. Müller-Buschbaum, Z. Bo, C. Yang, Z. Luo, *Angew. Chem., Int. Ed.* **2024**, *63*, 202315625.
[12] H. Chen, Z. Zhang, P. Wang, Y. Zhang, K. Ma, Y. Lin, T. Duan, T. He, Z. Ma, G. Long, C. Li, B. Kan, Z. Yao, X. Wan, Y. Chen, *Energy Environ. Sci.* **2023**, *16*, 1773.
[13] Y. Wang, Z. Zheng, J. Wang, X. Liu, J. Ren, C. An, S. Zhang, J. Hou, *Adv. Mater.* **2023**, *35*, 2208305.
[14] R. Ma, H. Li, T. A. Dela Peña, X. Xie, P. W.-K. Fong, Q. Wei, C. Yan, J. Wu, P. Cheng, M. Li, G. Li, *Adv. Mater.* **2024**, *36*, 2304632.
[15] J. Wang, F. Bi, L. Du, C. Shang, S. Liu, Z. Du, D. Yu, X. Bao, *Adv. Funct. Mater.* **2024**, *34*, 2313850.
[16] B. Pang, C. Liao, X. Xu, L. Yu, R. Li, Q. Peng, *Adv. Mater.* **2023**, *35*, 2300631.
[17] L. Chen, J. Yi, R. Ma, L. Ding, T. A. Dela Peña, H. Liu, J. Chen, C. Zhang, C. Zhao, W. Lu, Q. Wei, B. Zhao, H. Hu, J. Wu, Z. Ma, X. Lu, M. Li, G. Zhang, G. Li, H. Yan, *Adv. Mater.* **2023**, *35*, 2301231.
[18] X. Yuan, Y. Zhao, D. Xie, L. Pan, X. Liu, C. Duan, F. Huang, Y. Cao, *Joule* **2022**, *6*, 647.
[19] B. Zou, W. Wu, T. A. Dela Peña, R. Ma, Y. Luo, Y. Hai, X. Xie, M. Li, Z. Luo, J. Wu, C. Yang, G. Li, H. Yan, *Nano-Micro Lett.* **2023**, *16*, 30.
[20] J. Chen, D. Li, M. Su, Y. Xiao, H. Chen, M. Lin, X. Qiao, L. Dang, X.-C. Huang, F. He, Q. Wu, *Angew. Chem., Int. Ed.* **2023**, *62*, 202215930.
[21] H. Gao, Y. Sun, L. Meng, C. Han, X. Wan, Y. Chen, *Small* **2023**, *19*, 2205594.
[22] L. Zhang, D. Deng, K. Lu, Z. Wei, *Adv. Mater.* **2024**, *36*, 2302915.
[23] J. Ge, L. Xie, R. Peng, Z. Ge, *Adv. Mater.* **2023**, *35*, 2206566.
[24] T. Xu, J. Lv, Z. Chen, Z. Luo, G. Zhang, H. Liu, H. Huang, D. Hu, X. Lu, S. Lu, C. Yang, *Adv. Funct. Mater.* **2023**, *33*, 2210549.
[25] Y. Gao, X. Yang, W. Wang, R. Sun, J. Cui, Y. Fu, K. Li, M. Zhang, C. Liu, H. Zhu, X. Lu, J. Min, *Adv. Mater.* **2023**, *35*, 2300531.
[26] H. Shen, Y. Xu, W. Zou, W. Zhang, J. Li, P. Cai, Y. Guo, H. Xu, X. Hao, Y. Sun, Y. Kan, Y. Yang, K. Gao, *Chem. Eng. J.* **2023**, *469*, 144063.
[27] Y. Liu, J. Zhang, C. Tian, Y. Shen, T. Wang, H. Zhang, C. He, D. Qiu, Y. Shi, Z. Wei, *Adv. Funct. Mater.* **2023**, *33*, 2300778.
[28] M. Jiang, H.-F. Zhi, B. Zhang, C. Yang, A. Mahmood, M. Zhang, H. Y. Woo, F. Zhang, J.-L. Wang, Q. An, *ACS Energy Lett.* **2023**, *8*, 1058.
[29] K. Ma, W. Feng, H. Liang, H. Chen, Y. Wang, X. Wan, Z. Yao, C. Li, B. Kan, Y. Chen, *Adv. Funct. Mater.* **2023**, *33*, 2214926.
[30] X. Wang, Z. Li, X. Zheng, C. Xiao, T. Hu, Y. Liao, R. Yang, *Adv. Funct. Mater.* **2023**, *33*, 2300323.
[31] W. Ye, Y. Yang, Z. Zhang, Y. Zhu, L. Ye, C. Miao, Y. Lin, S. Zhang, *Sol. RRL* **2020**, *4*, 2000258.
[32] J.-W. Lee, C. Sun, J. Lee, D. J. Kim, W. J. Kang, S. Lee, D. Kim, J. Park, T. N.-L. Phan, Z. Tan, F. S. Kim, J.-Y. Lee, X. Bao, T.-S. Kim, Y.-H. Kim, B. J. Kim, *Adv. Energy Mater.* **2024**, *14*, 2303872.
[33] Y. Bai, Z. Zhang, Q. Zhou, H. Geng, Q. Chen, S. Kim, R. Zhang, C. Zhang, B. Chang, S. Li, H. Fu, L. Xue, H. Wang, W. Li, W. Chen, M. Gao, L. Ye, Y. Zhou, Y. Ouyang, C. Zhang, F. Gao, C. Yang, Y. Li, Z.-G. Zhang, *Nat. Commun.* **2023**, *14*, 2926.
[34] H. Zhuo, X. Li, J. Zhang, S. Qin, J. Guo, R. Zhou, X. Jiang, X. Wu, Z. Chen, J. Li, L. Meng, Y. Li, *Angew. Chem., Int. Ed.* **2023**, *62*, 202303551.
[35] R. Sun, T. Wang, Q. Fan, M. Wu, X. Yang, X. Wu, Y. Yu, X. Xia, F. Cui, J. Wan, X. Lu, X. Hao, A. K. Y. Jen, E. Spiecker, J. Min, *Joule* **2023**, *7*, 221.
[36] R. Ma, Q. Fan, T. A. Dela Peña, B. Wu, H. Liu, Q. Wu, Q. Wei, J. Wu, X. Lu, M. Li, W. Ma, G. Li, *Adv. Mater.* **2023**, *35*, 2212275.
[37] Z. Zhang, D. Deng, Y. Li, J. Ding, Q. Wu, L. Zhang, G. Zhang, M. J. Iqbal, R. Wang, J. Zhang, X. Qiu, Z. Wei, *Adv. Energy Mater.* **2022**, *12*, 2102394.

[38] X. Ma, C. Wang, D. Deng, H. Zhang, L. Zhang, J. Zhang, Y. Yang, Z. Wei, *Small* **2023**, *n/a*, 2309042.
[39] J. Han, H. Xu, S. H. K. Paleti, Y. Wen, J. Wang, Y. Wu, F. Bao, C. Yang, X. Li, X. Jian, J. Wang, S. Karuthedath, J. Gorenflot, F. Laquai, D. Baran, X. Bao, *ACS Energy Lett.* **2022**, *7*, 2927.
[40] Z. Peng, K. Xian, Y. Cui, Q. Qi, J. Liu, Y. Xu, Y. Chai, C. Yang, J. Hou, Y. Geng, L. Ye, *Adv. Mater.* **2021**, *33*, 2106732.
[41] T. Wang, M.-S. Niu, Z.-C. Wen, Z.-N. Jiang, C.-C. Qin, X.-Y. Wang, H.-Y. Liu, X.-Y. Li, H. Yin, J.-Q. Liu, X.-T. Hao, *ACS Appl. Mater. Interfaces* **2021**, *13*, 11134.
[42] C. Guan, C. Xiao, X. Liu, Z. Hu, R. Wang, C. Wang, C. Xie, Z. Cai, W. Li, *Angew. Chem., Int. Ed.* **2023**, *62*, 202312357.
[43] Z. Fu, J.-W. Qiao, F.-Z. Cui, W.-Q. Zhang, L.-H. Wang, P. Lu, H. Yin, X.-Y. Du, W. Qin, X.-T. Hao, *Adv. Mater.* **2024**, *36*, 2313532.
[44] Q. Chen, H. Huang, D. Hu, C. Zhang, X. Xu, H. Lu, Y. Wu, C. Yang, Z. Bo, *Adv. Mater.* **2023**, *35*, 2211372.
[45] S. Zhang, F. Bi, J. Han, C. Shang, X. Kang, X. Bao, *Nano Energy* **2022**, *102*, 107742.
[46] W. Gao, R. Ma, T. A. Dela Peña, C. Yan, H. Li, M. Li, J. Wu, P. Cheng, C. Zhong, Z. Wei, A. K. Y. Jen, G. Li, *Nat. Commun.* **2024**, *15*, 1946.
[47] W. Tang, Z. Ding, Y. Su, Q. Weng, Y. Zhang, R. Li, W. Huang, Z. Wang, Y. Wu, Y. Han, K. Zhao, Z. Yang, X. Wang, S. Liu, *Adv. Funct. Mater.* **2024**, *34*, 2312289.
[48] Y. Liang, D. Zhang, Z. Wu, T. Jia, L. Lüer, H. Tang, L. Hong, J. Zhang, K. Zhang, C. J. Brabec, N. Li, F. Huang, *Nat. Energy* **2022**, *7*, 1180.
[49] Y. Bai, Z. Zhang, Q. Zhou, H. Geng, Q. Chen, S. Kim, R. Zhang, C. Zhang, B. Chang, S. Li, H. Fu, L. Xue, H. Wang, W. Li, W. Chen, M. Gao, L. Ye, Y. Zhou, Y. Ouyang, C. Zhang, F. Gao, C. Yang, Y. Li, Z.-G. Zhang, *Nat. Commun.* **2023**, *14*, 2926.
[50] C. Wang, X. Ma, Y.-f. Shen, D. Deng, H. Zhang, T. Wang, J. Zhang, J. Li, R. Wang, L. Zhang, Q. Cheng, Z. Zhang, H. Zhou, C. Tian, Z. Wei, *Joule* **2023**, *7*, 2386.
[51] H. Zhuo, X. Li, J. Zhang, C. Zhu, H. He, K. Ding, J. Li, L. Meng, H. Ade, Y. Li, *Nat. Commun.* **2023**, *14*, 7996.
[52] W. Liu, H. Zhang, S. Liang, T. Wang, S. He, Y. Hu, R. Zhang, H. Ning, J. Ren, A. Bakulin, F. Gao, J. Yuan, Y. Zou, *Angew. Chem., Int. Ed.* **2023**, *62*, 202311645.
[53] Z. Li, Z. Zhang, H. Chen, Y. Zhang, Y.-Q.-Q. Yi, Z. Liang, B. Zhao, M. Li, C. Li, Z. Yao, X. Wan, B. Kan, Y. Chen, *Adv. Energy Mater.* **2023**, *13*, 2300301.
[54] R. Ma, Y. Tao, Y. Chen, T. Liu, Z. Luo, Y. Guo, Y. Xiao, J. Fang, G. Zhang, X. Li, X. Guo, Y. Yi, M. Zhang, X. Lu, Y. Li, H. Yan, *Sci China Chem* **2021**, *64*, 581.
[55] Y. Jiang, X. Dong, L. Sun, T. Liu, F. Qin, C. Xie, P. Jiang, L. Hu, X. Lu, X. Zhou, W. Meng, N. Li, C. J. Brabec, Y. Zhou, *Nat. Energy* **2022**, *7*, 352.
[56] T. P. Chaney, A. J. Levin, S. A. Schneider, M. F. Toney, *Mater. Horiz.* **2022**, *9*, 43.
[57] J. Xin, W. Li, Y. Zhang, Q. Liang, C. Song, Y. Zhao, Z. He, J. Liu, W. Ma, *Battery Energy* **2023**, *2*, 20220040.
[58] X. Jiang, A. J. Gillett, T. Zheng, X. Song, J. E. Heger, K. Sun, L. V. Spanier, R. Guo, S. Liang, S. Bernstorff, P. Müller-Buschbaum, *Energy Environ. Sci.* **2023**, *16*, 5970.
[59] W. Wei, C. Zhang, Z. Chen, W. Chen, G. Ran, G. Pan, W. Zhang, P. Müller-Buschbaum, Z. Bo, C. Yang, Z. Luo, *Angew. Chem., Int. Ed.* **2024**, *63*, 202315625.
[60] R. Ma, C. Yan, P. W.-K. Fong, J. Yu, H. Liu, J. Yin, J. Huang, X. Lu, H. Yan, G. Li, *Energy Environ. Sci.* **2022**, *15*, 2479.
[61] K. Gao, W. Deng, L. Xiao, Q. Hu, Y. Kan, X. Chen, C. Wang, F. Huang, J. Peng, H. Wu, X. Peng, Y. Cao, T. P. Russell, F. Liu, *Nano Energy* **2016**, *30*, 639.
[62] Q. Zhao, H. Lai, H. Chen, H. Li, F. He, *J. Mater. Chem. A* **2021**, *9*, 1119.
[63] Y. Tamai, Y. Murata, S.-i. Natsuda, Y. Sakamoto, *Adv. Energy Mater.* **2024**, *14*, 2301890.
[64] T. A. Dela Peña, R. Ma, Z. Xing, Q. Wei, J. I. Khan, R. M. Young, Y. Hai, S. A. Garcia, X. Zou, Z. Jin, F. L. Ng, K. L. Yeung, D. F. Swearer, M. R. Wasielewski, J. Wang, H. Cha, H. Yan, K. S. Wong, G. Li, M. Li, J. Wu, *Energy Environ. Sci.* **2023**, *16*, 3416.
[65] Y. Xu, J. Wang, H. Yao, P. Bi, T. Zhang, J. Xu, J. Hou, *Chin. J. Chem.* **2023**, *41*, 1045.
[66] S.-i. Natsuda, T. Saito, R. Shirouchi, Y. Sakamoto, T. Takeyama, Y. Tamai, H. Ohkita, *Energy Environ. Sci.* **2022**, *15*, 1545.
[67] H. Chen, D. Hu, Q. Yang, J. Gao, J. Fu, K. Yang, H. He, S. Chen, Z. Kan, T. Duan, C. Yang, J. Ouyang, Z. Xiao, K. Sun, S. Lu, *Joule* **2019**, *3*, 3034.
[68] J. Qin, C. An, J. Zhang, K. Ma, Y. Yang, T. Zhang, S. Li, K. Xian, Y. Cui, Y. Tang, W. Ma, H. Yao, S. Zhang, B. Xu, C. He, J. Hou, *Sci. China Mater.* **2020**, *63*, 1142.
[69] M. Riede, D. Spoltore, K. Leo, *Adv. Energy Mater.* **2021**, *11*, 2002653.
[70] W. Wang, C. Zeng, N. Tsubaki, *Green Carbon* **2023**, *1*, 133.